Beneficial aerodynamic effect of wing scales on the climbing flight of butterflies

IOP Publishing Bioinspir. Biomim. 12 (2017) 016013 doi:10.1088/1748-3190/aa551d

Bioinspiration & Biomimetics

PAPER

RECEIVED
9 August 2016

REVISED
6 December 2016

ACCEPTED FOR PUBLICATION
21 December 2016

PUBLISHED
30 January 2017

Beneficial aerodynamic effect of wing scales on the climbing flight of butterflies

Nathan Slegers[1], Michael Heilman[1], Jacob Cranford[2], Amy Lang[3], John Yoder[4] and Maria Laura Habegger[5]

[1] Department of Mechanical Engineering, George Fox University, Newberg, OR 97132, USA
[2] Gloyer-Taylor Laboratories LLC, 112 Mitchell Blvd. Tullahoma, TN 37388, USA
[3] Department of Aerospace Engineering and Mechanics, University of Alabama, Tuscaloosa, AL 35487, USA
[4] Department of Biological Sciences, University of Alabama, Tuscaloosa, AL 35487, USA
[5] Department of Integrative Biology, University of South Florida, Tampa, FL 33620, USA

E-mail: nslegers@georgefox.edu

Keywords: Butterfly, insects, surface patterning, unsteady aerodynamics, flapping, aerodynamic efficiency

Abstract

It is hypothesized that butterfly wing scale geometry and surface patterning may function to improve aerodynamic efficiency. In order to investigate this hypothesis, a method to measure butterfly flapping kinematics optically over long uninhibited flapping sequences was developed. Statistical results for the climbing flight flapping kinematics of 11 butterflies, based on a total of 236 individual flights, both with and without their wing scales, are presented. Results show, that for each of the 11 butterflies, the mean climbing efficiency decreased after scales were removed. Data was reduced to a single set of differences of climbing efficiency using are paired *t*-test. Results show a mean decrease in climbing efficiency of 32.2% occurred with a 95% confidence interval of 45.6%–18.8%. Similar analysis showed that the flapping amplitude decreased by 7% while the flapping frequency did not show a significant difference. Results provide strong evidence that butterfly wing scale geometry and surface patterning improve butterfly climbing efficiency. The authors hypothesize that the wing scale's effect in measured climbing efficiency may be due to an improved aerodynamic efficiency of the butterfly and could similarly be used on flapping wing micro air vehicles to potentially achieve similar gains in efficiency.

1. Introduction

The area of bio-inspired engineering has only just begun to make vital discoveries. Insects in particular, while being the subject of study for decades [1, 2], can still yield many untold breakthroughs. The rapidly developing field of micro air vehicles (MAVs) has recently created a surge in the study of insect flight for biomimicry. Recent progress in low Reynolds numbers ($10–10^4$) flapping flight and unsteady aerodynamics has shown that increases in generated lift can be achieved [2, 3]. Insect flight kinematics have also been extensively investigated, providing tools to develop dynamic models for flapping wing MAVs and validation for advancing aerodynamic theories [4, 5].

Butterflies and their scales have been extensively studied for their optical properties [6] as well as for their super-hydrophobic nature [7]. However, the aerodynamic benefit of the surface patterning resulting from the scale microgeometry shown in figure 1 has yet to be fully documented. While there exists a misconception that butterflies need their scales to fly, no reasonable aerodynamic explanation as to how the scales benefit the butterfly has been proven and accepted. Within a given species, scale size only varies proximodistally. Recent work has shown that the scales on the hindwing of the Blue Pansy (*Junonia orithya*), an aggressive flyer, generally decrease in size from the wing base towards the edge [8]. This reduction in scale size can be as much as 40%, and the reason for this occurrence was attributed to a maturation wave derived from morphogenetic factors emanating from the postbasal hinge region. However, no real biological function for the size decrease was proposed. Rather, the principle function of the morphogenetic wave was hypothesized to regulate scale coloration while consequently affecting scale size [8]. The fact that higher velocities would be induced towards the tip in flapping flight suggests that the scale geometry and surface patterning may function to improve aerodynamic efficiency of the butterfly.

Nachtigal [9] was one of the first to consider the beneficial aerodynamic effect of butterfly scales and

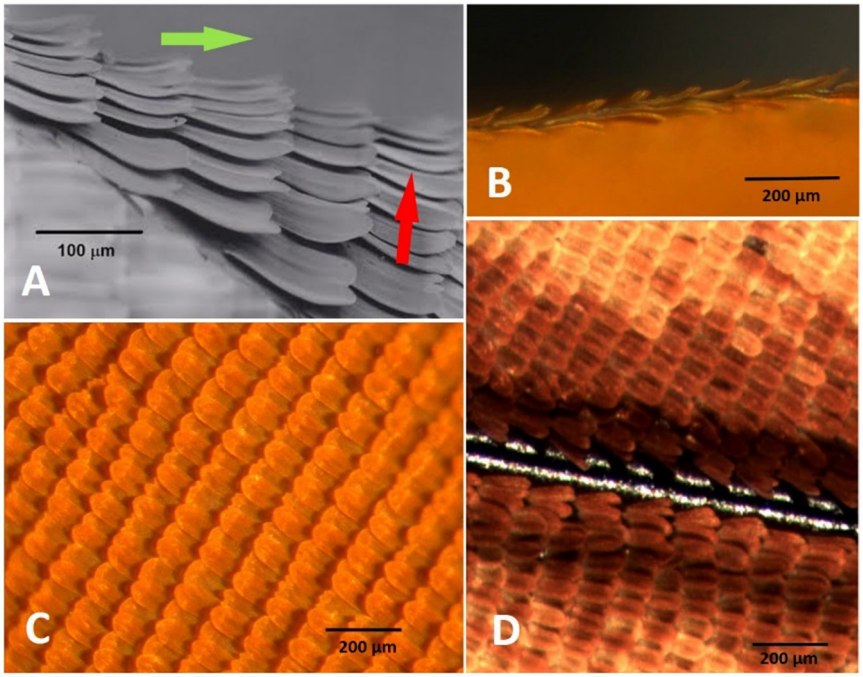

Figure 1. (A) Monarch butterfly dorsal scales imaged using SEM. (B) Sagitall cut through wing showing scales. (C) Dorsal view of orange Monarch scales. (D) Monarch dorsal scales showing how they form in rows perpendicular to the veins on the wing.

attempted to determine the lift and drag on dead specimens under gliding conditions in a wind tunnel experiment. His results indicated increased lift of 15% with the presence of the scales. Later research by Chebbi and Tavoularis [10], and Savoie and Gangno [11], began to look at low Reynolds number experiments and simulations to study the vortex formation within a triangular cavity modeled after the shingle-like pattern observed on butterfly scales. This research documented vortex formation at various Reynolds numbers but failed to adequately resolve any aerodynamic function of the scales [11].

Surface patterning such as dimples and riblets have similarities to butterfly scales and are well-known. The use of small dimples, such as on a golf ball, are known to delay flow separation and thereby decrease the pressure drag. However, dimples do more than just trip the boundary layer to the turbulent state. It has been shown by Choi *et al* [12], that the formation of embedded cavity vortices, or small localized regions of separation within the surface that allow the outer boundary layer flow to skip over the dimples, is a crucial aspect to this mechanism of separation delay and results in a wider Re range of decreased drag than generic roughness elements. Riblets (ridges) or streamwise grooves, first inspired by the grooves found on shark denticles [13], have been demonstrated as a passive mechanism to decrease turbulent skin friction drag. Bechert *et al* [14] performed exhaustive experiments with optimizing riblet spacing and cavity geometry resulting in a riblet tape for application to aircraft capable of a local 8% reduction in skin friction drag. Another approach considered the consequences of a partial-slip condition over a 2D transverse ribbed surface, first conjectured by Bushnell [15] as a possible means of achieving drag reduction (a flow phenomenon he referred to as the 'micro-air bearing' effect). However, Savill [16] later observed that a turbulent boundary layer forming above the surface caused fluid to enter and leave the cavities resulting in an overall increase in surface drag. Experimental studies on axisymmetric bodies with 2D transverse grooves have resulted in a measureable reduction in form drag [17] where they attributed separation control to the formation of the embedded vortices obviating the no-slip condition.

This work further investigates how microgeometry from surface patterning of butterfly scales may contribute to flight performance. The flight of a butterfly is a very complex flow, for the wings are used to generate thrust and lift while also generating drag. If the animal accelerates or increases its overall potential energy, as in the upward flights in this study, then the impeding forces of drag and weight are less than the thrust and lift. The sources of drag can come from three components: skin friction drag, pressure drag and induced drag. Induced drag is a drag due to lift and is seen as the energy of the vortices shed into the wake. If scale microgeometry contributes to a very low Re 'roller bearing effect' whereby fluid is trapped between the scales and forms embedded vortices, the outer flow would pass over the scales potentially decreasing the component of friction drag resulting in an increased flight efficiency (figure 1(a)). Conversely, flow passing over the scales in the direction of the rows could increase skin friction drag, but there exist regions during flight where this would be advantageous. For instance, in the vicinity of the leading-edge vortex [2], a key component of insect flight responsible for approximately two-thirds of the

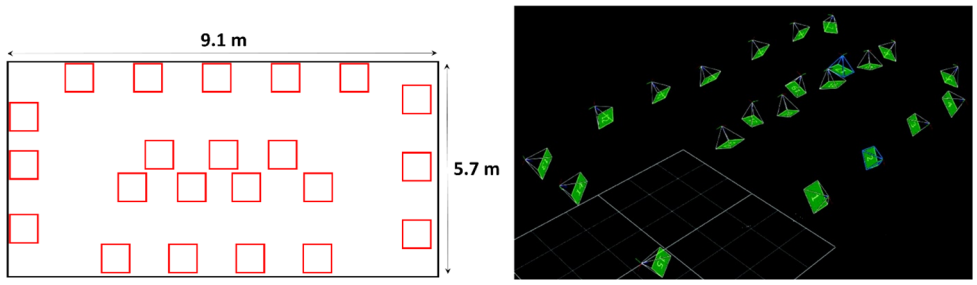

Figure 2. Top view of camera location (left) and camera orientation (right).

lift, such a mechanism could be used to retard vortex growth and increase friction drag in the direction along that wing that potentially contributes to both thrust and lift. At the same time the energy of the leading edge vortex shed into the wake could also be reduced (i.e. a kind of wake capture mechanism), thereby decreasing the component of induced drag while also permitting the vortex to stay attached longer. Such an effect may be felt by the butterfly and result in a change in flapping frequency or amplitude. If the scales are aligned along the wings to benefit from these effects, overall aerodynamic efficiency could be increased.

In order to document how the flight efficiency of butterflies is impacted by scales, the work presented here compares the free-flight body kinematics and flapping of butterflies with and without wing scales using new high speed motion capture techniques. Video was first utilized by Jensen [18] to film the tethered flight of a locust in order to measure kinematics of the wings and determine the aerodynamic forces. However, it was observed that tethering of locust could significantly reduce the wing beat frequency requiring new methods for measuring kinematics insect flight to be developed [19]. Experiments have since evolved to use videography to capture kinematic data of specimens in hovering flight [20–22]. A primary challenge associated with using conventional videography to capture kinematic data of insect flight is that it must maintain a regulated trajectory through a small volume in view of the cameras. Pioneering work was typically limited to images from only a few cameras, used extremal stimuli such as lights to induce desire motion within wind tunnels [19–24], and required extensive numerical processing to calculate the location of each point of interest [25–29]. These methods typically result in a small size of the capture volume, which restricts the number of flaps captured in sequence to typically less than five, and processing rates which restrict the number of flapping sequences that can be processed.

In this work a different approach is taken where 22 high speed motion tracking cameras are used in a 150 m^3 (5.7 m $\times$ 9.1 m $\times$ 3.0 m) capture volume. The large volume provides enough space for unobstructed butterfly flight over a large sequence of flaps without requiring any extra equipment to entice flight. Using the large number of cameras allows capture of both wing flapping and body motion with millimeter accuracy. This technique was used to record a total of 236 unobstructed climbing flights from 11 different Monarch butterflies (*Danaus plexipus*), with and without scales. Mean climbing efficiencies, flapping angles, and amplitude variations were calculated for each butterfly in order to document how butterfly wing scale geometry and surface patterning may function to improve overall flight efficiency.

2. Methods

2.1. Butterfly motion capture system

Optical tracking of all butterflies in this study was accomplished using 22 VICON T40 cameras with a 64° Field of View, 12.5 mm lense, and 2352 $\times$ 1728 resolution. Each camera is equipped with a near infrared (NIR) strobe and visible light filters. The cameras track reflective markers specifically designed for motion capture systems and efficiently reflect the NIR light. Each camera contains an onboard processer which locates all markers in a frame and estimates the markers' centroid. When two or more cameras can locate a marker, the marker's 3D position can be identified. The accuracy of the estimated location depends on both the proximity of the marker to the cameras (resulting image resolution) and the number of cameras able to detect each marker. These two factors make camera setup within the desired capture volume critical to the quality of data to be collected.

For this study, all 22 cameras were located at the top of a 5.7 m $\times$ 9.1 m $\times$ 3.0 m capture volume. Specific locations of the cameras are shown in figure 2 where camera positions are marked as boxes. Camera orientations are shown in the virtual environment image in right side of figure 2. The actual capture volume is shown in figure 3 where netting was used to prevent the butterflies from escaping. The high density of cameras within the large capture volume enables data to be capture while also providing long segments of unrestricted free flight butterfly trajectories.

2.2. Reflective markers and monarch butterflies

Tracking the motion of a butterfly requires knowing both the position of the thorax (body) and left and right fore wings. The flapping angle γ is defined as the angle formed by the left fore wing apex, thorax, and the right fore wing apex as shown in figure 4. A single reflective

Figure 3. Capture volume.

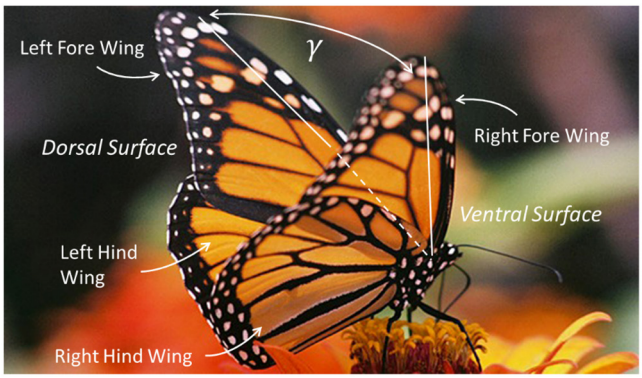

Figure 4. Butterfly geometry.

marker on the thorax and three pairs of reflective markers on the wings were required to capture the butterfly kinematics. The three pairs of wing markers located at the left fore wing apex, right fore wing apex, and right hind wing are shown in figure 5. Each pair of markers consists of markers on both the dorsal and ventral side at each location. Pairs were used because as the butterfly wings close while up ($\gamma = 0$), markers on the dorsal side are obscured. Likewise as the wings close while down ($\gamma = 2\pi$), markers on the ventral side are hidden. In order to minimize weight, custom 3 mm $\times$ 5 mm flat markers, designed to reflect NIR light efficiently, and weighing 5.8 mg were used. The combined 7-marker system mass is close to 40 mg, or only about 8% the mass of an average 500 mg butterfly.

2.3. Testing procedures

Experiments described below were developed to gather data comparing the flight of butterflies with scales and with their scales removed. Butterflies were provided by Shady Oak Butterfly Farm and delivered in individual envelopes surrounded by ice packs to ensure the butterflies remained dormant prior to testing. Monarch butterflies use cool temperatures during wintering to maintain lipid reserves. This reduced activity state was used to safely handle, measure and place markers on the specimens. Prior to test preparation, each butterfly was placed in terrariums under a lamp and allowed to rest and feed. During test preparation, each butterfly was then chilled and kept cold as they were first weighed, then had markers placed and were weighed again. The butterflies were then again placed in terrariums under a lamp and allowed to rest overnight to reduce the potential effects of stress from handling and the addition of markers. Butterfly sex was recorded and equal numbers of female and male butterflies were tested in order to control for potential variations due to gender. All results reported indicate the gender of each butterfly for completeness, however, no significant differences were identified based on gender during testing.

On the day of testing butterflies were removed from the terrariums one at a time and the method of random cluster sampling was taken where flights were recorded for 10 consecutive motion capture tests. A test consisted of releasing the butterfly in the middle of the capture volume and recording a trial lasting 20 s. No external stimulus was provided since the butterflies naturally flew away when released. After trial data was recorded, the butterfly was captured in preparation for another test. When every butterfly had been recorded

Figure 5. NIR wing marker placement.

Figure 6. Removal of scales from an experimental specimen.

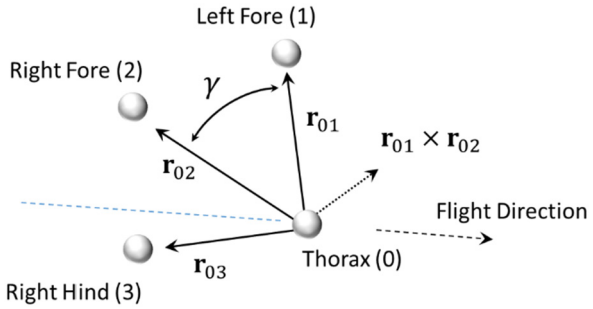

Figure 7. Butterfly flapping geometry definitions.

in an initial round of 10 tests, the butterflies were put through a second round of 10 flight tests. After both rounds of flight tests were completed the butterflies were placed back in the terrarium. It was noted that temperature had a noticeable effect on the butterfly flights. As temperatures increase, the length of time the butterflies flew without trying to land increased. For consistency, temperature in the test volume was maintained at 75°F for all tests.

To compare the effect scales have on butterfly flight, the wing scales of previously measured Monarchs were removed. Scale removal is shown in figure 6 where they are brushed from the wings and the reflective markers replaced. Scales were removed after the initial tests with scales were completed and the markers were replaced in their original positions. The median reduction in mass after scales were removed for all butterflies tested was 9.5%. However, it must be noted that the removal of scales were not a significant contributor to the reduction in mass. Rather, all butterflies were allowed to feed freely prior to each test preparation. Therefore, the variation in mass was primarily due to variations in feeding patterns and the consumption of fluids. As with the original tests the de-scaled butterflies were then placed in terrariums and allowed to rest overnight before repeating the testing procedure for the butterflies without scales. All effort was made to incur no additional damage to the wings other than to remove the scales. In some cases specimens were damaged (wing tips torn or wing veins broken) and these specimens where not used for flight testing.

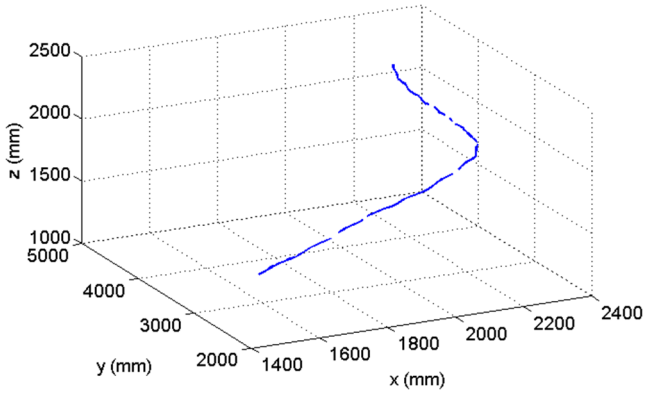

Figure 8. Butterfly 2 3D trajectory (with scales).

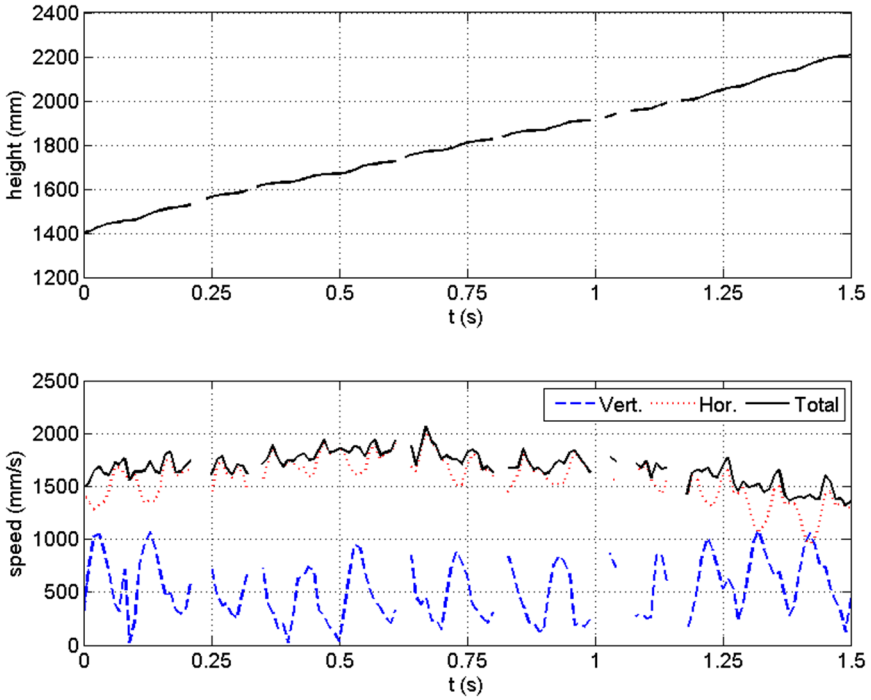

Figure 9. Butterfly 2 trajectory (with scales).

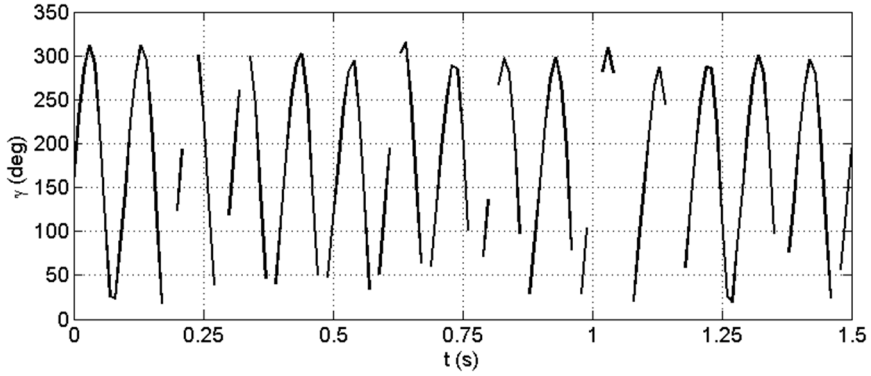

Figure 10. Butterfly 2 flapping angle (with scales).

2.4. Butterfly flapping geometry

The motion capture system, at each time sample, reports the 3D position of each of the four reflective markers in the capture volume's global reference frame. The four markers: thorax, left fore wing, right fore wing, and right hind wing are labeled 0–3, respectively. Three wing vectors are defined in figure 7 using the thorax as a reference. Each wing vector is

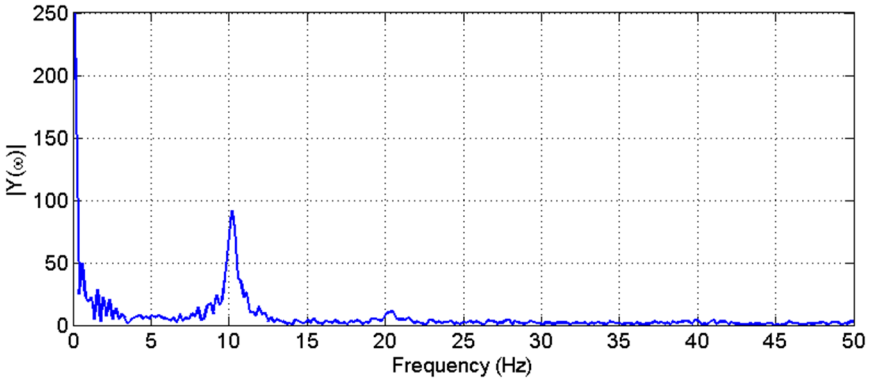

Figure 11. Butterfly 2 flapping angle FFT (with scales).

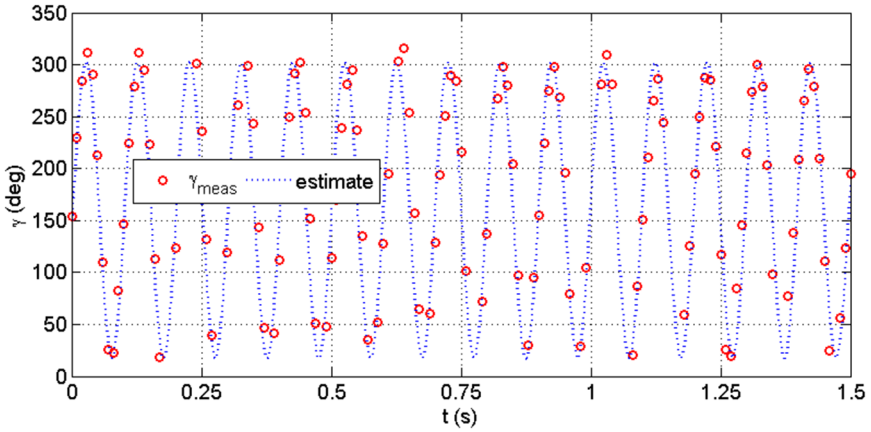

Figure 12. Estimated butterfly 30 flapping angle model.

found by simply subtracting the thorax reference marker from each wing's marker position. The flapping angle γ can be found using (1) which uses both the cross product and dot product definitions and the two fore wing vectors.

However, since the norm of the cross product is used in (1), there is an ambiguity that occurs between flapping angles less than π and those greater than π. This ambiguity can be resolved by noting that because of the fore wing marker locations, when γ is less than π, the resulting cross product of r_{01} and r_{02} will point towards the flight direction. When γ is greater than π the same cross product will point towards the hind wings. As a result, using the hind marker vector r_{03}, the condition in (2) will be less than zero when γ is less than π and greater than zero when γ is greater than π.

$$\tan\gamma = \frac{|r_{01} \times r_{02}|}{r_{01} \cdot r_{02}} \quad (1)$$

$$r_{03} \cdot (r_{01} \times r_{02}) \quad (2)$$

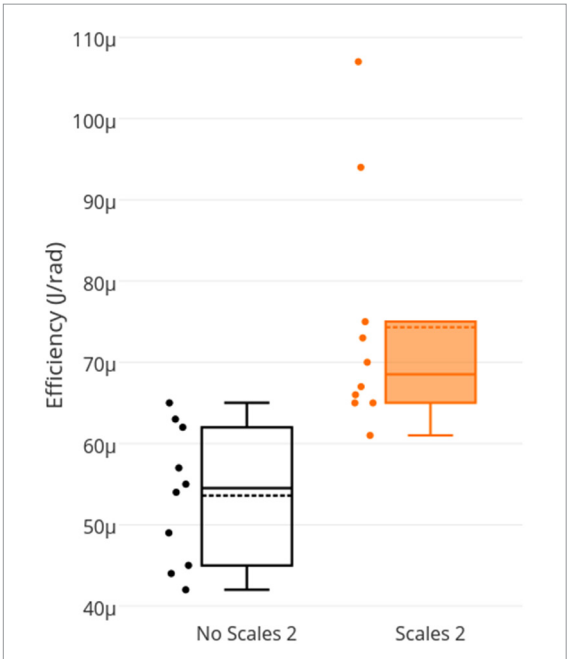

Figure 13. Butterfly 2 scales versus no scales climbing efficiency box plot.

2.5. Butterfly trajectory analysis

All butterfly marker trajectories were recorded at 100–250 Hz. A sample trajectory for butterfly 2 which spans approximately 15 complete wing flaps over a 1.5 s climbing flight (with scales) is shown in figures 8 and 9. Trajectories, height, and speeds shown in figures 8 and 9 are specifically for marker 0 (thorax) while the flapping angle in figure 10 is calculated using (1) and (2). Short gaps appear in figures 8 and 9 at 0.23, 0.33,

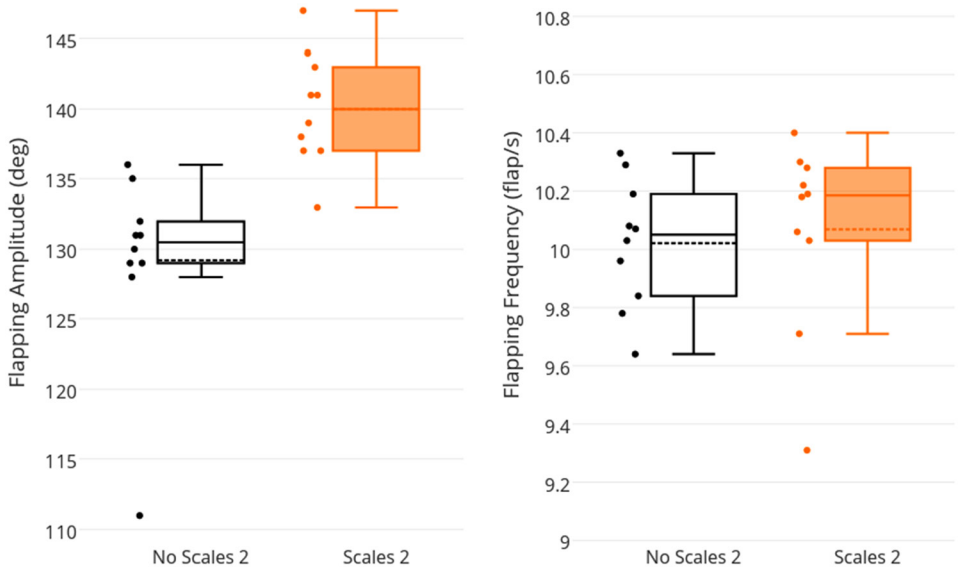

Figure 14. Butterfly 2 scales versus no scales flapping amplitude and frequency box plot.

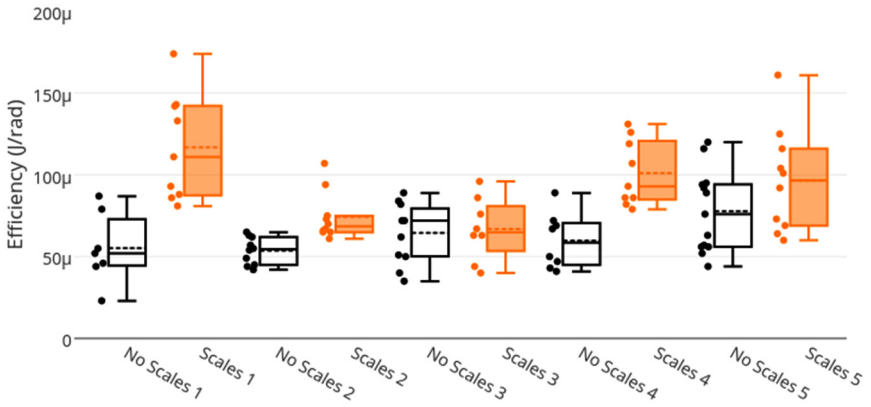

Figure 15. All female butterfly scales versus no scales box plots.

0.62, 0.80, 1.0, and 1.15 s. These gaps occur as the thorax marker is obscured from the cameras during the butterfly's dynamic maneuvers and wing flapping. The vertical velocity oscillates during flapping as the thorax moves down and up as the wings flap open and closed. Likewise, the horizontal velocity oscillates as the generated lift and drag change, with the horizontal velocity reaching a maximum as the wings close (γ approaches zero). Oscillations in the total 3D speed are much smaller.

Gaps occur in the flapping angle data more often and for longer segments than the height or speed since data for all four markers must be present to complete the calculations in (1) and (2). Segments without flapping data are particularly pronounced as the wings close toward the top of a flapping cycle (γ approaching zero.) The loss of data near $\gamma = 0$ is due to markers 1 and 2 converging on each other which makes distinguishing between them difficult. In many instances the motion capture system tries to treat the two markers in proximity as a single marker. Despite having some gaps in the flapping angle, it is apparent from figure 10 that the flapping angle follows a sinusoidal trajectory. The Fast Fourier Transform (FFT) of γ, shown in figure 11, confirms that the flapping kinematics are primarily of a single frequency, 10.2 flaps s^{-1}.

In order to form an estimation of the flapping amplitude, γ, and frequency despite missing many segments, it is assumed that the flapping kinematics can be modeled as the following four parameter function

$$\gamma = A\sin(\omega t + \phi) + B \tag{3}$$

where, A, ω, ϕ, and B are constants to be estimated for each trajectory. An initial estimate for each of the four parameters is found using

$$B_0 = \overline{\gamma}_{\text{meas}}, \tag{4}$$

$$A_0 = \max(|\gamma_{\text{meas}} - B_0|), \tag{5}$$

ω_0 as the FFT frequency, and ϕ_0 as the average ϕ resulting from using (3) with A_0, B_0, and ω_0 for the first four data points. A two parameter unconstrained optimization problem can be created by forming the error vector

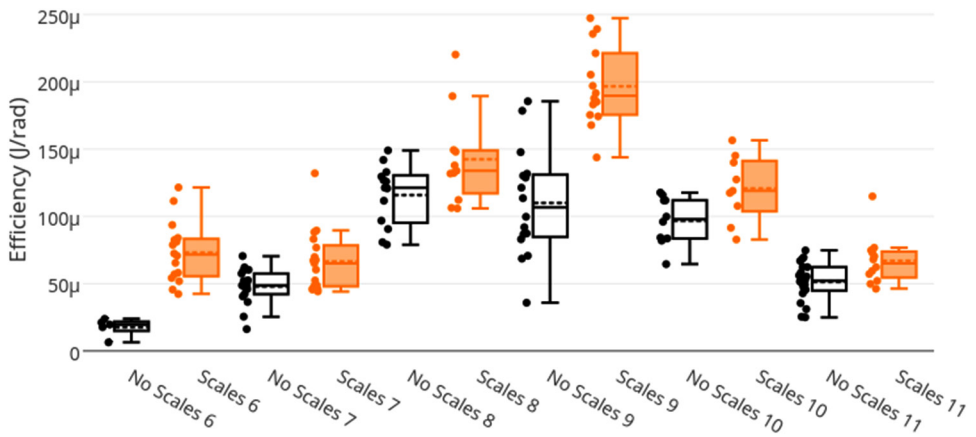

Figure 16. All male butterfly scales versus no scales box plots.

Table 1. Summary for climbing efficiency.

Butterfly	Sex	Mean η_{climb} (μJ rad^{-1}) Scales	No scales	% Δ η_{climb}	Confidence interval Δ η_{climb} (μJ rad^{-1})
1	F	116	55.0	−53.2	93–31
2	F	74.4	53.8	−27.6	32–9
3	F	66.8	64.4	−3.59	21 to −16
4	F	101	59.8	−40.7	61–22
5	F	96.4	77.6	−19.6	44 to −6
6	M	73.2	17.7	−75.7	77–34
7	M	66.6	47.9	−27.9	31–6
8	M	142	116	−18.7	51–2
9	M	197	110	−44.0	113–60
10	M	121	96.7	−19.9	45–3
11	M	67.1	51.5	−23.1	27–4

$$\mathbf{e} = \boldsymbol{\gamma}_{meas} - [\widetilde{A}\sin(\widetilde{\omega}\boldsymbol{t}_{meas} + \phi_0) + B_0] \quad (6)$$

where, $\widetilde{A}$ and $\widetilde{\omega}$ are estimates of the two parameters in (3), $\boldsymbol{\gamma}_{meas}$ and $\boldsymbol{t}_{meas}$ are measured data, and B_0 and ϕ_0 remain constant. The Nelder–Mead Simplex method [30] is then used to find parameter estimates $\widetilde{A}$ and $\widetilde{\omega}$, starting with the initial values A_0 and ω_0, that minimize

$$J = \mathbf{e}^T\,\mathbf{e} + N(\widetilde{A} - A_0)^2 \quad (7)$$

with N being the number data points. The first term in (7) is the squared error summation while the second term limits variation from the initial amplitude estimate and is used to increase estimation robustness. Estimation robustness was also improved by performing the optimization using only the upper and lower 20% of measured flapping angles.

The estimated flapping motion, using the proposed technique, is shown in figure 12 where the final estimates of $\widetilde{A}$, B_0, and $\widetilde{\omega}$ are 142.5°, 159.6°, and 10.04 flaps s^{-1}, respectively.

In order to compare the effect that scales have on monarch butterfly flight, it is necessary to define a flight performance metric that can be evaluated with and without scales. For any climbing flight segment,

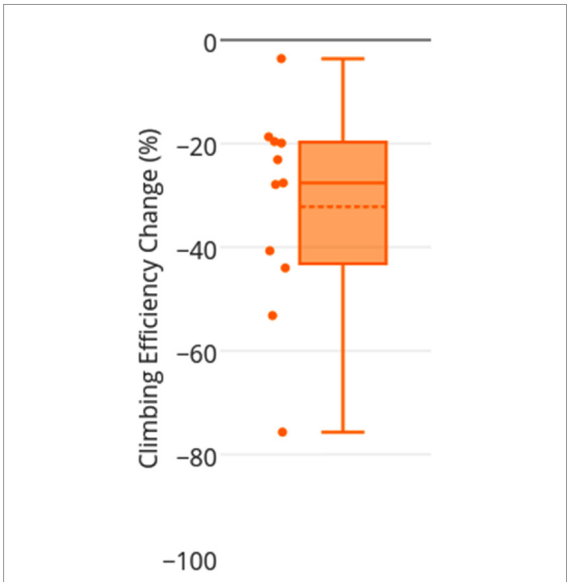

Figure 17. Efficiency change for all butterflies with scales removed.

the increase in energy over that segment can be calculated by determining the total energy (potential and kinetic) at both the initial and final stages. Comparison of different length trajectories and butterflies, requires that the energy change be normalized with respect to both the number of wings flaps occurring over the entire trajectory and the average flapping amplitude. The resulting climbing flight efficiency is defined as the average energy required per flapping radian and can be written as

$$\eta_{climb} = \frac{m\left[\frac{1}{2}(v_f^2 - v_i^2) + g(h_f - h_i)\right]}{\widetilde{\omega}(t_f - t_i)\widetilde{A}} \quad (8)$$

The climbing flight efficiency has units of J rad^{-1}, where the speeds used are the total 3D speed of marker 0 (thorax) and m is the butterfly mass, including markers. Strictly speaking, (8) is not a conventional efficiency formed by the ratio of output work to input power. Rather, as defined in (8), the climbing efficiency is the average induced climbing energy produced per radian

Table 2. Summary for climbing flapping amplitude.

Butterfly	Sex	Max–mean–min amplitude (°)		% Δ mean	Confidence interval Δ amplitude (°)
		Scales	No scales		
1	F	155–134–115	141–129–117	−4.0	16.3 to −5.7
2	F	147–140–133	136–129–111	−8.3	16.2–5.4
3	F	145–134–125	134–126–117	−6.4	14.1–1.7
4	F	142–133–116	136–127–122	−4.3	12.9 to −1.5
5	F	140–133–119	128–125–121	−6.0	11.8–4.0
6	M	159–137–126	135–113–96	−17.3	34.1–13.4
7	M	142–134–127	139–125–109	−6.3	13.4–3.5
8	M	151–141–132	150–134–111	−5.5	16.0 to −0.4
9	M	145–136–126	143–128–111	−5.8	13.6–2.3
10	M	142–132–116	128–121–105	−7.9	18.3–2.5
11	M	126–119–110	126–113–94	−5.2	11.9–0.5

of flapping. In fact, in steady level flight with constant velocity and height, the numerator of (8) may be zero. For this study, only climbing flights were investigated where, climbing was defined as a trajectory where the average height increase to trajectory length ratio was greater than 10%. Applying (8) to butterfly 2, which has a mass of 516 mg, results in an η_{climb} of 74.4 μJ rad^{-1} over the 1.5 s trajectory shown in figures 8–10.

3. Results and discussion

3.1. Single butterfly mean efficiency, flapping frequency, and amplitude calculation

Investigation of potential changes in climbing flight efficiencies that may result from the removal of scales was accomplished by finding the mean climbing efficiency of a butterfly, first with scales and then without scales. Based on the butterfly's mean efficiencies, the percent difference in mean without scales compared to the mean with scales, called %Δ η_{climb}, can be found. It is assumed that a specific butterfly's population of all climbing flights will have a normal distribution of climbing efficiencies with some mean. Therefore, for a specific butterfly, two independent populations are defined. The first being all climbing flights of the butterfly with scales and the second being all climbing flights of the butterfly with scales removed. The data collected for butterfly 2, 10 with scales and 10 with no scales, represent the two independent samples from the two populations. Figure 13 shows box plots for the calculated efficiency of 20 climbing flights for butterfly 2. The end of the boxes represent the upper and lower quartiles, while the whiskers show the largest and smallest efficiencies not more than 1.5 box-lengths from the box. Sample medians and means are shown by the solid and dashed lines, respectively, within the boxes. Individual data points are shown by the markers.

Climbing efficiency means for butterfly 2 are 53.8 μJ rad^{-1} without scales and 74.4 μJ rad^{-1} with scales. The result is a mean decrease in climbing efficiency of 20.6 μJ/flap, or a % Δ η_{climb} of −27.6%, for butterfly 2 when scales were removed. A two-sample t-test ($n = 18$) results in the 95% confidence interval for the decrease in climbing efficiency for butterfly 2 of 32–9 μJ rad^{-1} (two sided p-value < 0.001). Results indicate a strong inference that butterfly 2 experiences a decrease in climbing efficiency when the scales are removed.

Table 3. Summary for climbing flapping frequency.

Butterfly	Sex	Mean freq. (flap s^{-1})		% Δ	Confidence interval Δ freq. (flap s^{-1})
		Scales	No scales		
1	F	9.95	9.49	−4.7	0.76–0.17
2	F	10.07	10.02	−0.5	0.31 to −0.22
3	F	10.31	9.84	−4.7	0.65–0.31
4	F	9.76	9.07	−7.1	0.96–0.41
5	F	9.48	9.53	0.5	−0.33–0.23
6	M	9.43	9.69	2.8	−0.65–0.13
7	M	9.93	10.56	6.3	−0.84 to −0.42
8	M	10.48	11.05	5.4	−0.97 to −0.18
9	M	10.43	10.07	−3.5	0.60–0.13
10	M	10.78	10.87	0.9	−0.31–0.12
11	M	9.70	10.08	3.9	−0.60 to −0.16

A similar procedure was completed for butterfly 2's flapping amplitude and frequency with results summarized in figure 14. The mean flapping amplitude decrease is 11.4° with a 95% confidence interval of 16.2–5.4° (two sided p-value < 0.001), strongly suggesting that butterfly 2 experiences a decrease in mean flapping amplitude when scales are removed. The mean frequency decrease is only 0.05 flaps s^{-1} with a 95% confidence interval of 0.31 to −0.22 flap s^{-1} (two sided p-value $= 0.5$), suggesting that scales have no impact of flapping frequency for butterfly 2.

3.2. Comparison of all butterflies with and without scales

Results for butterfly 2 strongly suggest that removing scales may decrease the climbing efficiency and amplitude while the flapping frequency may see no change for that particular butterfly. Similar tests

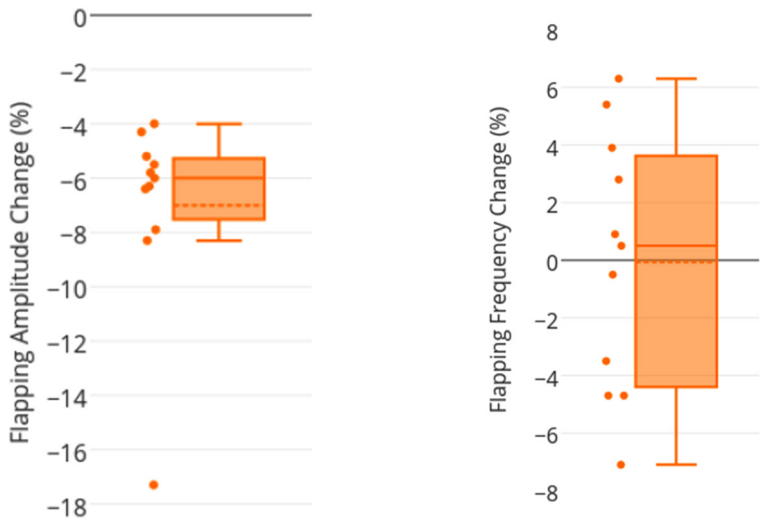

Figure 18. Flapping amplitude (left) and frequency (right) change for scales versus no scales.

calculating the mean climbing efficiencies were completed on a total of 11 butterflies, 5 females and 6 males, totaling 236 individual flights. Figures 15 and 16 show the side by side comparisons for climbing efficiency of each of the 11 butterflies, separated by sex, with the mean efficiencies and their percent changes given in table 1.

Table 1 shows that all 11 butterflies experienced a decrease in the mean climbing efficiency when scales were removed. The climbing efficiency for all 11 butterflies was dominated by the potential energy increase during climbing while, of the 236 individual flights, nearly half experienced only a small increase in velocity while the others experienced a small velocity decrease. Figure 17 summarizes in a box plot the percent changes in climbing efficiency for all 11 flights. Considering the 11 butterflies with and without scales as a paired t-test ($n = 10$), where the data is reduced to single set of differences, the mean change in climbing efficiency is -32.2%. The 95% confidence interval is found to be -45.6% to -18.8% with a p-value less than 0.001, which provides strong evidence that the climbing efficiency decreases when scales are removed.

Tables 2 and 3 provide a summary of the statistical results of flapping amplitude and frequency for the 11 butterflies. Similar to the climbing efficiency results, the peak-to peak flapping amplitude decreases for all 11 butterflies. Figure 18 summarizes the amplitude results as a paired t-test ($n = 10$) in which the set's mean change in amplitude is -7.0%. The 95% confidence interval is -9.5% to -4.6% with a two-sided p-value < 0.001, which provides strong evidence that the flapping amplitude decreases when scales are removed. Table 3 and figure 18 show convincing evidence that removing scales has no effect to the flapping frequency and that the data is consistent with the null hypothesis of no change in flapping frequency. Six of the 11 butterflies demonstrate a small increase in frequency while five show a small decrease. The set's mean change in flapping frequency is -0.07 flap s^{-1} with a 95% confidence interval of -3.1% to 2.9% flap s^{-1}.

4. Conclusion

Statistical results are presented for the climbing flight flapping kinematics of 11 butterflies (5 female and 6 male), both with and without their wing scales. In order to investigate the hypothesis that wing scales provide a beneficial aerodynamic effect, a climbing flight efficiency parameter that measured the energy increase induced by wing flapping was defined and measured experimentally using optical tracking methods.

Results showed that for each of the 11 butterflies, the mean climbing efficiency decreased after scales were removed. Forming a paired t-test from each butterfly's flights with scales and without, the data was reduced to a single set of percent differences. The paired t-test showed a mean decrease in climbing efficiency of 32.2% with a 95% confidence interval of 45.6%–18.8% (two-sided p-value < 0.001). Similar analysis showed that the flapping amplitude decreased by 7% while the flapping frequency remained statistically unchanged. Combined, the results provide strong evidence that scale geometry and surface patterning may function to improve wing aerodynamic efficiency of the butterflies. Flapping kinematic results suggest that as the climbing efficiency decreases with the scales removed, the butterflies maintain the same flapping frequency but must reduce flapping amplitude due to the increased work load to climb. One possible explanation for this phenomenon is that butterflies have a preferred flapping frequency, but as their efficiency is reduced, they must reduce their flapping amplitude to compensate, similar to a pedestrian who reduces their stride on an incline. The findings presented suggest that geometry and surface patterning similar to that found on Monarch butterflies may be able to be applied to MAV's

and other man made flapping vehicles to achieve similar increases in efficiency.

Acknowledgments

This material is based upon work supported by the National Science Foundation: Division of Chemical, Bioengineering, Environmental, and Transport Systems: CBET-1335848 and CBET-1335572.

References

[1] Sun M 2014 Insect flight dynamics: stability and control *Rev. Mod. Phys.* **86** 615–46
[2] Shyy W, Aono H, Kang C-K and Liu H 2013 *An Introduction to Flapping Wing Aerodynamics* (New York: Cambridge University Press)
[3] Shyy W, Aono H, Chimakurthi S K, Trizila P, Kang C K, Cesnik C E S and Liu H 2010 Recent progress in flapping wing aerodynamics and aeroelasticity *Prog. Aerosp. Sci.* **46** 284–327
[4] Chen M W, Zhang Y L and Sun M 2013 Wing and body motion and aerodynamic and leg forces during take-off in droneflies *J. R. Soc. Interface* **10** 20130808
[5] Mou X L, Liu Y P and Sun M 2011 Wing motion measurement and aerodynamics of hovering true hoverflies *J. Exp. Biol.* **214** 2832–44
[6] Ingram A 2009 *Functional Surfaces in Biology* (Berlin: Springer) ch 15
[7] Fang Y, Gang S, Cong Q, Chen G and Ren L 2008 Effects of methanol on wettability of the non-smooth surface on butterfly wing *J. Bionic Eng.* **5** 127–33
[8] Kusaba K and Otaki J 2009 Positional dependence of scale size and shape in butterfly wings: wing-wide phenotypic coordination of color-pattern elements and background *J. Insect Phys.* **55** 175–83
[9] Nachtigall W 1967 Aerodynamische Messungen am Tragfluegelsystem segeinder Schmetterlinge *Z. Vgl. Physiol.* **54** 210
[10] Chebbi B and Tavoularis S 1990 Low Reynolds number flow in and above asymmetric, triangular cavities *Phys. Fluids* A **2** 1044
[11] Savoi R and Gagno Y 1995 Numerical simulation of the flow over a model of the cavities on a butterfly wing *J. Therm. Sci.* **4** 185
[12] Choi J, Jeon W and Choi H 2006 Mechanism of drag reduction by dimples on a sphere *Phys. Fluids* **18** 1–4
[13] Lang A, Motta P, Hueter R, Habegger M L and Afroz F 2011 Shark skin separation control mechanisms *Marine Tech. Soc. J.* **45** 208–15
[14] Bechert D W, Bruse M, Hage W, Van der Hoeven J and Hoppe G 1997 Experiments on drag-reducing surfaces and their optimization with an adjustable geometry *J. Fluid Mech.* **338** 59–87
[15] Bushnell D 1983 Turbulent drag reduction for external flows *AIAA* Paper 83-0227
[16] Savill A 1988 A flow visualization investigation of turbulent boundary layer structure overmicro air bearing surfaces including effect of outer layer manipulation *2nd Int. Symp. on Fluid Control, Measurement Mechanics and Flow Visualization* pp 430–6
[17] Howard F and Goodman W 1985 Axisymmetric bluff-body drag reduction through geometrical modification *J. Aircraft* **22** 516–22
[18] Jensen M 1956 Biology and physics of locust flight. III. The aerodynamics of locust flight *Proc. R. Soc.* B **239** 511–52
[19] Willmott A P and Ellington C P 1997 The mechanics of flight in the hawkmoth *Manduca sexta J. Exp. Biol.* **2722** 2705–22
[20] Wang Z J 2005 Dissecting insect flight *Annu. Rev. Fluid Mech.* **37** 183–210
[21] Weis-Fogh T 1973 Quick estimates of flight fitness in hovering animals, including novel mechanisms for lift production *J. Exp. Biol.* **59** 169–230
[22] Dudley R and Ellington C P 1990 Mechanics of forward flight in bumblebees: I. Kinematics and morphology *J. Exp. Biol.* **148** 19–52
[23] Srygley R B and Thomas A L R 2002 Unconventional lift-generating mechanisms in free-flying butterflies *Nature* **420** 487–9
[24] Tanaka H and Shimoyama I 2010 Forward flight of swallowtail butterfly with simple flapping motion *Bioinspir. Biomim.* **5** 026003
[25] Ristroph L, Berman G J, Bergou A J, Wang Z J and Cohen I 2009 Automated hull reconstruction motion tracking (HRMT) applied to sideways maneuvers of free-flying insects *J. Exp. Biol.* **212** 1324–35
[26] Walker S M, Thomas A L R and Taylor G K 2009 Photogrammetric reconstruction of high-resolution surface topographies and deformable wing kinematics of tethered locusts and free-flying hoverflies *J. R. Soc. Interface* **6** 351–66
[27] Lin T, Zheng L, Hedrick T and Mittal R 2012 The significance of moment-of-inertia variation in flight manoeuvres of butterflies *Bioinspir. Biomim.* **7** 044002
[28] Zheng L, Hedrick T L and Mittal R 2013 Time-varying wing-twist improves aerodynamic efficiency of forward flight in butterflies *PLoS One* **8** 1–10
[29] Zheng L, Wang X, Khan A, Vallance R and Mittal R 2009 A combined experimental-numerical study of the role of wing flexibility in insect flight *47th AIAA Aerospace Science Meeting* pp 1–10
[30] Lagarias J, Reeds J, Wright M and Wright P 1998 Convergence properties of the nelder-mead simplex method in low dimensions *SIAM J. Optim.* **9** 112–47